Nuclear Engineering and Technology 49 (2017) 1451–1456

Contents lists available at ScienceDirect

Nuclear Engineering and Technology

journal homepage: www.elsevier.com/locate/net

Original Article

A preliminary study of pilot-scale electrolytic reduction of UO_2 using a graphite anode

Sung-Wook Kim*, Dong Hyun Heo, Sang Kwon Lee, Min Ku Jeon, Wooshin Park, Jin-Mok Hur, Sun-Seok Hong, Seung-Chul Oh, Eun-Young Choi

Pyroprocessing Division, Korea Atomic Energy Research Institute, 989-111 Daedeok-daero, Yuseong-gu, Daejeon 34057, Republic of Korea

ARTICLE INFO

Article history:
Received 6 March 2017
Received in revised form
12 May 2017
Accepted 23 May 2017
Available online 13 June 2017

Keywords:
Anode
Carbon
Electrolytic Reduction
Pilot Scale
Pyroprocessing
Spent Fuel

ABSTRACT

Finding technical issues associated with equipment scale-up is an important subject for the investigation of pyroprocessing. In this respect, electrolytic reduction of 1 kg UO_2, a unit process of pyroprocessing, was conducted using graphite as an anode material to figure out the scale-up issues of the C anode-based system at pilot scale. The graphite anode can transfer a current that is 6–7 times higher than that of a conventional Pt anode with the same reactor, showing the superiority of the graphite anode. UO_2 pellets were turned into metallic U during the reaction. However, several problems were discovered after the experiments, such as reaction instability by reduced effective anode area (induced by the existence of Cl_2 around anode and anode consumption), relatively low metal conversion rate, and corrosion of the reactor. These issues should be overcome for the scale-up of the electrolytic reducer using the C anode.

1. Introduction

Electrolytic reduction is a key technique in pyroprocessing, which is being developed to manage and recycle spent fuels generated in pressurized water reactors [1–3]. Spent fuels, a complex mixture of metal oxides (mainly UO_2), are electrochemically converted to metallic states [e.g., $UO_2 = U + 2O_2(g)$] after electrolytic reduction using LiCl–Li_2O molten salt as an electrolyte [1–3]. Pt has been widely used as an anode material evolving O_2 gas ($2O^{2-} = O_2(g) + 4e^-$) [4–7]. However, it has been identified that the Pt anode is gradually damaged during the operation owing to (electro)chemical side reactions [5–7]. The cost of the raw material of Pt is extremely high, and thus its limited lifetime is a major hurdle for pyroprocessing.

Several candidates have been extensively investigated to replace the Pt anode [8–16]. Among these, C is an attractive material because of its low cost and reasonable electrical and mechanical properties [14–16]. Under moderate operation conditions (~3.0 V) based on the CO/CO_2 evolution reaction ($C + xO^{2-} = CO_x + 2xe^-$) of the C anode, accumulation of the Li_2CO_3 by-product in the LiCl–Li_2O electrolyte cannot be prohibited, which makes the reuse of the electrolyte impossible [14,17]. Recently, a high-voltage electrolytic reduction technique was proposed using the C anode in small-scale experiments (up to 50 g UO_2) [15]. The dissociation voltage of LiCl [$2LiCl = 2Li + Cl_2(g)$] is approximately 3.46 V [14]. When a sufficiently high voltage is applied, Cl_2 is expected to be evolved preferentially at the C anode instead of O_2 and CO/CO_2 [15]. In the presence of Cl_2, Li_2CO_3, which is the major side reaction product of the C anode, can be removed via various chemical reaction pathways [15]. At the same time, metallic Li formed at the cathode assists the reduction of UO_2 to metallic U ($UO_2 + 4Li = U + 4Li_2O$) [15]. It has been confirmed that the high-voltage operation effectively prevents Li_2CO_3 accumulation, meaning that the electrolyte can be reused [15].

Scale-up is an important issue for the commercialization of pyroprocessing [1]. In this study, preliminary test of the electrolytic reduction of 1 kg UO_2 was performed using graphite as the C anode. Three experiments were conducted to examine its feasibility and to verify the technical issues associated with scale-up. An identical reactor, which was used to investigate the Pt anode at the 1-kg scale, was used to compare the cell's performance [18].

2. Materials and methods

An electrolytic reducer was installed inside an Ar-filled glove box to prevent air and O_2 exposure. Further description of the

* Corresponding author.
E-mail address: swkim818@kaeri.re.kr (S.-W. Kim).

http://dx.doi.org/10.1016/j.net.2017.05.004

electrolytic reducer is given in the literature [18]. The electrolytic reducer can be equipped with one cathode and two anodes as shown in Fig. 1A. A stainless steel basket (STS 314L) with a perforated wall was used as the cathode (Fig. 1B). UO_2 pellets (1 kg) were loaded into the cathode basket (length × width × height = 100 × 25 × 120 mm). The electrochemical performance of two types of rod-shaped graphite anodes (diameter = 8 mm and length = 20 cm/diameter = 15 mm and length = 10 cm) (R8500; SGL Carbon group, Wiesbaden, Germany) was examined. The graphite anode was held by a stainless steel lead as shown in Fig. 1C. The anode shroud was made with a 3 wt.% MgO-stabilized ZrO_2 tube (bottom) (outer/inner diameter = 28/22 mm) and stainless steel pipe (top) (Fig. 1D). The effect of the anode shroud was investigated by controlling the immersion depth. The initial electrolyte used was dehydrated LiCl (6 kg) (99%; Alfa Aesar, Ward Hill, United States of America) without any additives. The reaction temperature was 650°C, which is high enough to melt the electrolyte. The LiCl was replenished after the reaction to maintain an adequate electrolyte height. The electrolytic reduction was carried out with a constant current operation using an external power supply (EX30-240; ODA Technologies, Incheon, Republic of Korea), and cell voltage was monitored with a digital multimeter (34405A; Agilent Technologies, Santa Clara, United States of America) simultaneously. The gas product evolved at the anode surface was exhausted through off-gas line connected to highly concentrated NaOH solution to eliminate the Cl_2 within it. The concentration of Li_2O and Li_2CO_3 in the electrolyte was determined by an autotitrator (G20; Mettler-Toledo, Greifensee, Switzeland) using 0.1N HCl solution. X-ray diffraction (XRD) (D8 Advance; Bruker) analysis was carried out for phase identification.

3. Results and discussion

3.1. Effect of anode shroud

Prior to the electrolytic reduction runs, the effect of the anode shroud was investigated using one graphite anode (diameter = 8 mm) as shown in Fig. 2. Electrochemical reaction was done with the constant current operation to keep the measured cell voltage at around 7.0 V. When the whole graphite anode was covered with the shroud (immersion depth = 4.5 cm), the electrochemical reaction was not stable and the cell voltage abruptly reached the voltage limit of the power supply within a few minutes (Fig. 2A). Such abnormal behavior was not observed in the small-scale experiment [15]. In this experiment, the cell current was 30 A, with a current density of 2.54 A/cm^2, which is higher than that observed in the small-scale experiment (~1.94 A/cm^2). It is speculated that the high current density increases the concentration of gas bubbles generated at the graphite anode. The gas bubbles would reduce the effective anode area and increase the anode overpotential significantly, preventing the sustenance of the electrochemical reaction. It is worth noting that the open-circuit voltage was approximately 3.3 V, comparable to the LiCl decomposition voltage, when the electrochemical reaction was stopped. This implies that a large amount of Cl_2 gas existed around the graphite anode inside the shroud, which was not properly removed. The existence of the Cl_2 gas around the anode should be negative on the reaction stability. It has been reported that Cl_2 bubbles tend to remain for a long time at the C anode in the LiCl–KCl electrolyte [19,20]. These suggest that removing Cl_2 bubbles around the anode is important for the application of the graphite anode.

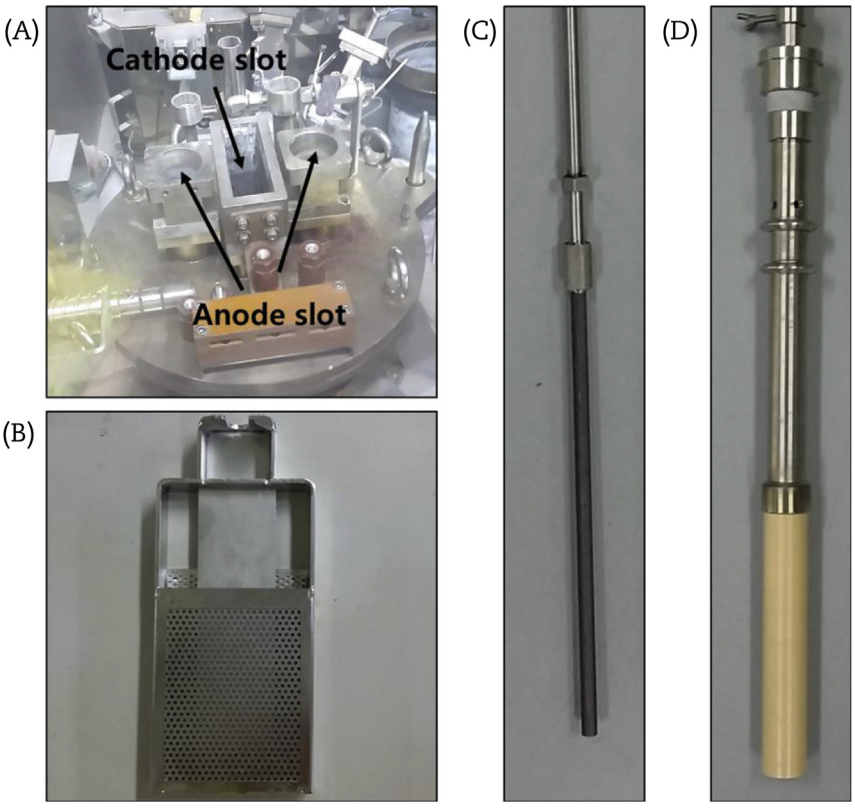

Fig. 1. Electrolytic reduction equipment. (A) Flange. (B) Cathode basket. (C) Graphite anode. (D) Anode shroud.

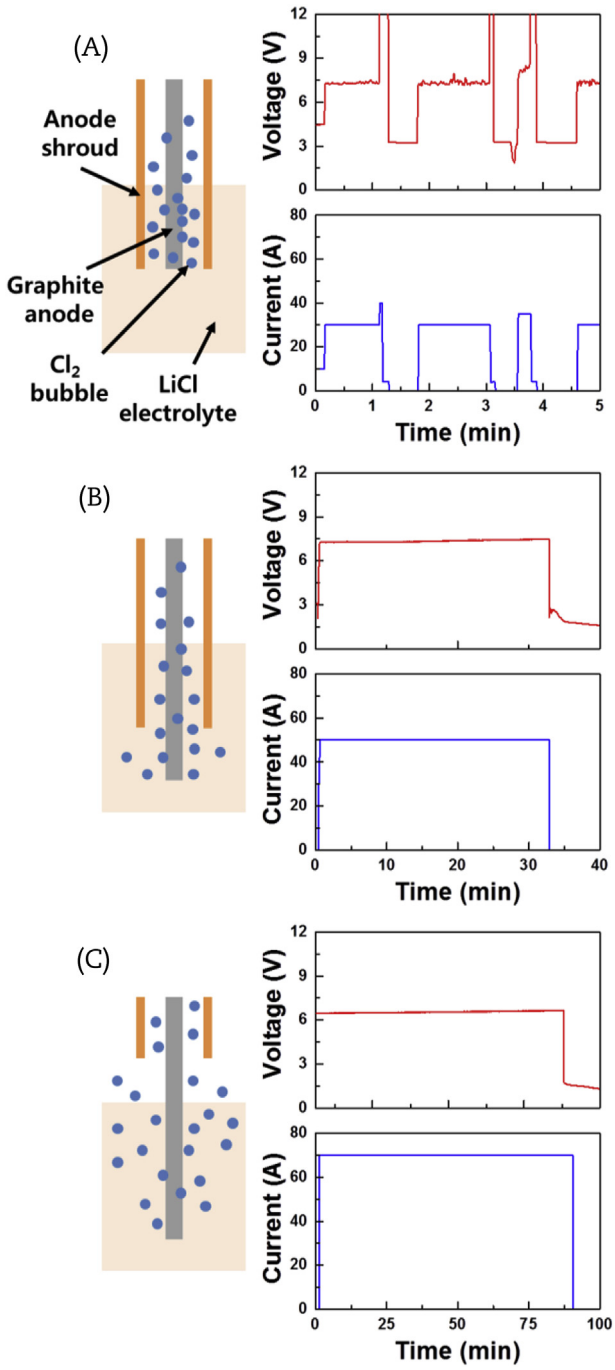

Fig. 2. Schematic diagram of the graphite anode and anode shroud position, and the corresponding current–voltage relationship. (A) Full coverage. (B) Partial coverage. (C) Noncoverage.

By contrast, the electrochemical reaction became remarkably stable, with increased cell current (50 A), when the graphite anode was partially exposed (anode immersion depth = 8 cm, shroud immersion depth = 4.5 cm) to the electrolyte (Fig. 2B). A higher cell current (70 A) was reached for more than 1 h when the shroud did not cover the graphite anode (anode immersion depth = 8 cm), as shown in Fig. 2C. The current densities in Figs. 2B and 2C were approximately 2.47 and 3.40 A/cm^2, respectively. As the anode area directly exposed to the electrolyte increases, the ionic motion

Table 1
Summary of the three electrolytic reduction experiments of 1 kg UO_2 using the graphite anode.

Batch	#1	#2	#3
No. of anodes	1	2	2
Anode diameter (mm)	8	8	15
Initial anode immersion depth (cm)	6.5	8	8
Initial anode area (cm^2)	16.8	41.2	78.9
Input charge to theoretical value (%)	150	130	165

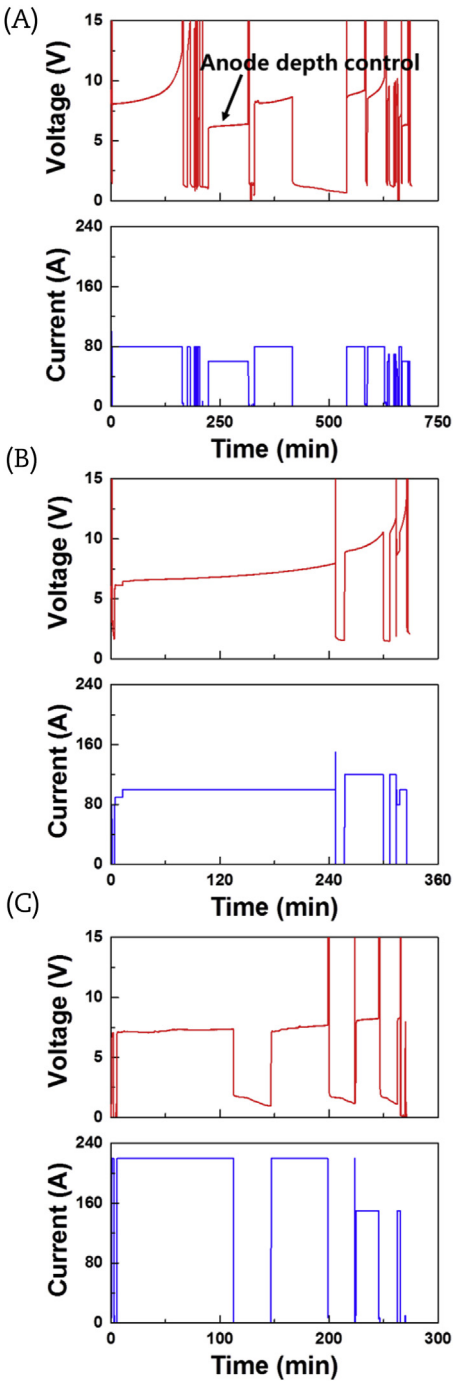

Fig. 3. Current–voltage diagram during electrolytic reduction for the three batches.

around the anode is enhanced, which increases the effective anode area, enabling high current operation. In addition, the Cl_2 bubbles escape easily from the anode to the opened space, as shown in the schematic illustration in Fig. 2, which is confirmed by the low open-circuit voltage. Depletion of Cl_2 bubbles near the anode decreases the anode overpotential, resulting in enhanced electrochemical activity at the anode. Cl_2 gas, however, may spread widely inside the reactor, leading to more corrosion when the anode is not covered with the shroud. Hence, a trade-off between the effective anode area and shroud position should be made. Using a porous ceramic shroud would be an effective way to secure both a large effective anode area, by enhancing ionic transport through open pores, and minimal Cl_2 escape.

3.2. Electrolytic reduction of UO_2

Electrolytic reduction of 1 kg UO_2 was performed to estimate cell performance for three batches with different anode configurations, as summarized in Table 1. A noncovering shroud was used in these experiments to improve reaction stability. Fig. 3 shows the current–voltage diagram of the three batches. Cell voltage gradually increased with time, and this behavior is more significant in the smaller anode area (Fig. 3A). This is because the graphite anode was gradually consumed to form CO/CO_2 during the prolonged reaction owing to the existence of O^{2-} ions (i.e., Li_2O) released from UO_2 to form metallic U. An abrupt voltage jump that halted the electrochemical reaction was observed alongside this anode consumption. Once the anode area reached its limit and the electrochemical reaction could no longer be sustained, the anode immersion depth was controlled to ensure a sufficient anode area, as indicated in Fig. 3A. The maximum cell current with the largest anode area was 220 A, as shown in Fig. 3C, which is much higher than that of the Pt anode system (35 A) examined in the same reactor [18]. It is believed that higher cell voltage and higher concentrations of major anions participating in the anodic reaction (Cl^- in the C anode vs. O^{2-} in the Pt anode) play a critical role in the enhancement of the cell current. The concentration of Li_2O and Li_2CO_3 was less than 0.2 wt.% after each batch as shown in Table 2, demonstrating the suppression of by-product accumulation in the electrolyte.

Table 2
Concentration of Li_2O and Li_2CO_3 in the electrolyte after the reaction.

Batch	#1	#2	#3
Li_2O concentration (wt.%)	0.1804	0.1417	0.0003
Li_2CO_3 concentration (wt.%)	0.1861	0.1745	0.1198

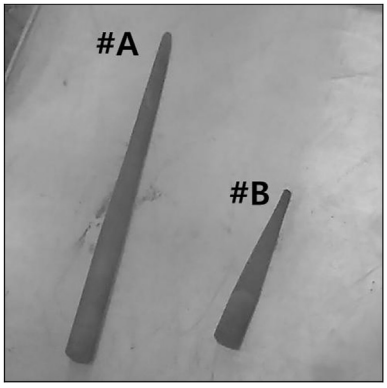

Fig. 4. Graphite anodes remaining after the reaction, showing that Anode #B is consumed more than Anode #A during the reaction (Batch #2).

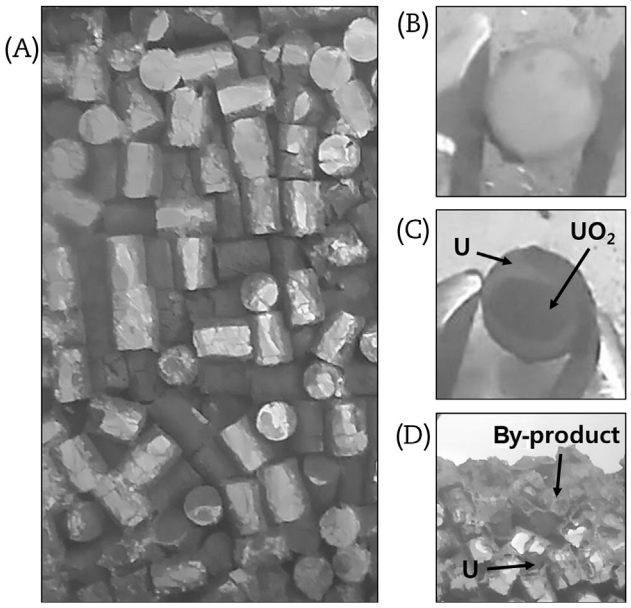

Fig. 5. Polished surface of the cathode products. (A) Group of pellets in the cathode basket. (B) Single pellet with full reduction. (C) Single pellet with partial reduction. (D) By-products located around the metallic U (Batch #3).

Interestingly, the two anodes were not consumed by the same amount during the reaction, as shown in Fig. 4. It is thought that Anode #A in Fig. 4 generated more Cl_2 and less CO/CO_2 than Anode #B in Fig. 4, or Anode #B might pass more current than Anode #A, resulting in the different consumption rate. Because various anions (e.g., Cl^-, O^{2-}, and CO_3^{2-}) exist together in the electrolyte, the anodic reaction can be varied (e.g., Cl_2, O_2, and CO/CO_2 evolution) according to the local environment surrounding each graphite anode. Additionally, it is almost impossible to make the two anodes have exactly the same potential owing to the difficulty in precisely controlling the iR drop, contact resistance, anode

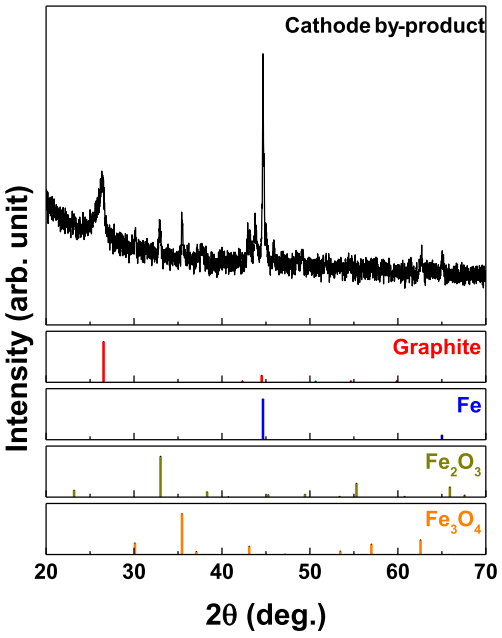

Fig. 6. XRD analysis of the cathode by-product after its dissolution into water.

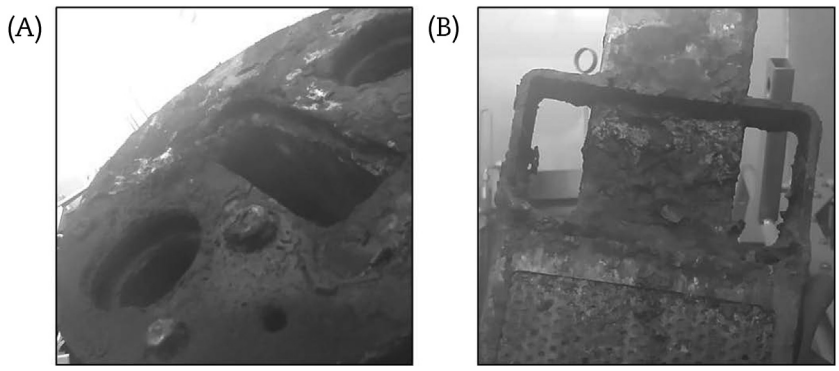

Fig. 7. Corrosion of the electrolytic reducer after the reaction. (A) Bottom plate of the flange. (B) Upper part of the cathode basket.

immersion depth, and so on. Therefore, slight differences in the anode potential can change the anodic reaction pathways. Hence, the anode consumption needs to be monitored periodically to keep the electrochemical reaction stable. This becomes more especially significant on a multielectrode system, which is expected to be used in the scale-up equipment.

Fig. 5 shows the cathode products after electrolytic reduction. The shiny, silver-colored surface of the cathode products can be seen after polishing, indicating that UO_2 pellets were reduced well to metallic U following the reaction (Figs. 5A and 5B). However, the core of several of the pellets remained as brown UO_2, as shown in Fig. 5C, despite the reaction supplying more than the theoretical charge given in Table 1. The limited diffusion rate of metallic Li into the UO_2 core through the reduced U surface decreases the conversion rate. The residual Li can then spread out from the cathode basket through the electrolyte. Hence, a longer rest interval where no current is applied would be required during the reaction to secure sufficient time for the Li to diffuse into the core. In addition, side reactions induced by Li_2CO_3 and corrosion products (e.g., $FeCl_x$ and FeO_x) in the electrolyte may consume supplied electrons, disturbing the metallic Li generation required for the reduction of UO_2. Indeed, cathode by-products were found in the cathode basket after the reaction, as shown in Fig. 5D. Most of these were dissolved in water, generating gas bubbles, and left a residual powder. This suggests that the major components are the frozen electrolyte (perhaps containing water-soluble $FeCl_x$) and the metallic Li, which forms H_2 bubbles in the water [$2Li + 2H_2O = H_2(g) + 2LiOH(aq)$]. Graphite, metallic Fe, Fe_2O_3, and Fe_3O_4 phases remaining in the by-product residue after dissolution were identified by X-ray diffraction analysis, as shown in Fig. 6. Graphite and metallic Fe can be formed by the electrochemical reduction of CO_3^{2-} ($CO_3^{2-} + 4e^- = C + 3O^{2-}$) [14] and Fe^{z+} ($Fe^{z+} + ze^- = Fe$) ions in the electrolyte to dissipate electrons. Fe_2O_3 and Fe_3O_4 are thought to be oxidation products of O_2 gas. O_2 can be electrochemically evolved at the anode ($2O^{2-} = O_2(g) + 4e^-$) or can be formed by chemical reaction between Li_2O and Cl_2 [$2Li_2O + 2Cl_2(g) = 4LiCl + 2O_2(g)$]. These by-product species may need to be removed by posttreatment (e.g., rinsing in clean LiCl molten salt) to minimize their effect on the subsequent processes.

Corrosion is a critical issue associated with the electrolytic reducer, which is mainly made of stainless steel. Fig. 7 shows that the reactor was severely damaged after the reaction. Because a noncovering shroud was used during its operation, the reactor was directly exposed to high-temperature Cl_2 in the presence of O_2, leading to corrosion at the metal surface. An effective off-gas system, including better anode shrouds, should be developed for the enhanced removal of corrosive gas phases inside the reactor. Attaching a ceramic plate or coating ceramic layer onto the surface of the metallic parts would also be useful to protect the reactor against corrosion.

4. Conclusion

A preliminary test of the electrolytic reduction of 1 kg UO_2 was performed with a graphite anode. UO_2 can be reduced to metallic U using the graphite anode with a maximum cell current of 220 A, which is remarkably improved from the Pt anode. Nevertheless, several issues still present challenges at this stage, and further investigation is required for the scale-up equipment including following:

- Development of an effective Cl_2 exhaustion system to maintain the stability of the electrochemical reaction and to minimize corrosion
- Development of a monitoring technique to measure anode consumption in order to maintain the stability of the electrochemical reaction
- Improvement of charge efficiency for the higher conversion rate of UO_2
- Examination of corrosion-resistant materials/coatings to extend the lifetime of the electrolytic reducer

Conflicts of interest

All authors declare no conflicts of interest.

Acknowledgments

This work was supported by the National Research Foundation of Korea (NRF) grant, funded by the Korean government (MISP) (2017M2A8A5015077).

References

[1] H.-S. Lee, G.-I. Park, K.-H. Kang, J.-M. Hur, J.-G. Kim, D.-H. Ahn, Y.-Z. Cho, E.-H. Kim, Pyroprocessing technology development at KAERI, Nucl. Eng. Technol. 43 bm (2011) 317–328.
[2] H. Ohta, T. Inoue, Y. Sakamura, K. Kinoshita, Pyroprocessing of light water reactor spent fuels based on an electrochemical reduction technology, Nucl. Technol. 150 (2005) 153–161.
[3] T. Inoue, L. Koch, Development of pyroprocessing and its future direction, Nucl. Eng. Technol. 40 (2008) 183–190.
[4] J.-M. Hur, S.M. Jeong, H.S. Lee, Underpotential deposition of Li in a molten LiCl–Li_2O electrolyte for the electrochemical reduction of U from uranium oxides, Electrochem. Commun. 12 (2010) 706–709.
[5] S.M. Jeong, H.-S. Shin, S.-H. Cho, J.-M. Hur, H.S. Lee, Electrochemical behavior of a platinum anode for reduction of uranium oxide in a LiCl molten salt, Electrochim. Acta 54 (2009) 6335–6340.

[6] Y. Sakamura, T. Omori, T. Inoue, Application of electrochemical reduction to produce metal fuel material from actinide oxides, Nucl. Technol. 162 (2008) 169–178.
[7] Y. Sakamura, T. Omori, Electrolytic reduction and electrorefining of uranium to develop pyrochemical reprocessing of oxide fuels, Nucl. Technol. 171 (2010) 266–275.
[8] S.-W. Kim, E.-Y. Choi, W. Park, H.S. Im, J.-M. Hur, TiN anode for electrolytic reduction of UO_2 in pyroprocessing, J. Nucl. Fuel Cycle Waste Technol. 13 (2015) 229–233.
[9] Y. Sakaumra, M. Iizuka, Applicability of nickel ferrite anode to electrolytic reduction of metal oxides in LiCl–Li_2O melt at 923 K, Electrochim. Acta 189 (2016) 74–82.
[10] S.-W. Kim, E.-Y. Choi, W. Park, H.S. Im, J.-M. Hur, A conductive oxide as an O_2 evolution anode for the electrolytic reduction of metal oxides, Electrochem. Commun. 55 (2015) 14–17.
[11] A. Merwin, D. Chidambaram, Alternative anodes for the electrolytic reduction of UO_2, Metall. Mater. Trans. A 46 (2015) 536–544.
[12] S.-W. Kim, W. Park, H.S. Im, J.-M. Hur, S.-S. Hong, S.-C. Oh, E.-Y. Choi, Electrochemical behavior of liquid Sb anode system for electrolytic reduction of UO_2, J. Radioanal. Nucl. Chem. 303 (2015) 1041–1046.
[13] S.-W. Kim, S.-K. Lee, H.W. Kang, E.-Y. Choi, W. Park, S.-S. Hong, S.-C. Oh, J.-M. Hur, Electrochemical properties of noble metal anodes for electrolytic reduction of uranium oxides, J. Radioanal. Nucl. Chem. 311 (2017) 809–814.
[14] J.-M. Hur, J.-S. Cha, E.-Y. Choi, Can carbon be an anode for electrochemical reduction in a LiCl–Li_2O molten salt? ECS Electrochem. Lett. 3 (2014) E5–E7.
[15] S.-W. Kim, M.K. Jeon, H.W. Kang, S.-K. Lee, E.-Y. Choi, W. Park, S.-S. Hong, S.-C. Oh, J.-M. Hur, Carbon anode with repeatable use of LiCl molten salt for electrolytic reduction in pyroprocessing, J Radional. Nucl. Chem. 310 (2016) 463–467.
[16] T. Biju Joseph, N. Sanil, K.S. Mohandas, K. Nagarajan, A study of graphite as anode in the electro-deoxidation of solid UO_2 in LiCl–Li_2O melts, J. Electrochem. Soc. 162 (2015) E51–E58.
[17] H.Y. Ryu, S.M. Jeong, Y.C. Kang, J.-G. Kim, Electrochemical carbon formation from a graphite anode in LiCl–Li_2O molten salt, Asian J. Chem. 25 (2013) 7019–7022.
[18] E.-Y. Choi, J. Lee, M.K. Jeon, S.-K. Lee, S.-W. Kim, S.-C. Jeon, J.H. Lee, J.-M. Hur, Electrolytic reduction of 1 kg-UO_2 in Li_2O–LiCl molten salt using porous anode shroud, J. Korean Electrochem. Soc. 18 (2015) 121–129 (in Korean).
[19] F. Lantelme, H. Alexopoulos, D. Devilliers, M. Chemla, A gas electrode: behavior of the chlorine injection electrode in fuse alkali chlorides, J. Electrochem. Soc. 138 (1991) 1665–1671.
[20] Y. Sakamura, M. Kurata, T. Inoue, Electrochemical reduction of UO_2 in molten $CaCl_2$ or LiCl, J. Electochem. Soc. 153 (2006) D31–D39.